Vitamin E - Phosphatidylethanolamine Interactions in Mixed Membranes with Sphingomyelin: Studies by ^{2}H NMR

Andres T. Cavazos, Jacob J. Kinnun[1], Justin A. Williams and Stephen R. Wassall*

Department of Physics, Indiana University-Purdue University, Indianapolis, IN 46202

*Email for correspondence: swassall@iupui.edu

[1] *Present address* Department of Medicinal Chemistry and Molecular Pharmacology, Purdue University, West Lafayette, IN 47907

This is the author's manuscript of the article published in final edited form as:

Cavazos, A. T., Kinnun, J. J., Williams, J. A., & Wassall, S. R. (2020). Vitamin E - phosphatidylethanolamine interactions in mixed membranes with sphingomyelin: Studies by 2H NMR. Chemistry and Physics of Lipids, 231, 104910. https://doi.org/10.1016/j.chemphyslip.2020.104910

Abstract

Among the structurally diverse collection of lipids that comprise the membrane lipidome, polyunsaturated phospholipids are particularly vulnerable to oxidation. The role of α-tocopherol (vitamin E) is to protect this influential class of membrane phospholipid from oxidative damage. Whether lipid-lipid interactions play a role in supporting this function is an unanswered question. Here, we compare the molecular organization of polyunsaturated 1-[$^2H_{31}$]palmitoyl-2-docosahexaenoylphosphatidylethanolamine (PDPE-d_{31}) and, as a control, monounsaturated 1-[$^2H_{31}$]palmitoyl-2-oleoylphosphatidylethanolamine (POPE-d_{31}) mixed with sphingomyelin (SM) and α-tocopherol (α-toc) (2:2:1 mol) by solid-state ^2H NMR spectroscopy. In both cases the effect of α-tocopherol appears similar. Spectral moments reveal that the main chain melting transition of POPE-d_{31} and PDPE-d_{31} is broadened beyond detection. A spectral component attributed to the formation of inverted hexagonal H_{II} phase in coexistence with lamellar L_α phase by POPE-d_{31} (20%) and PDPE-d_{31} (18%) is resolved following the addition of α-toc. Order parameters in the remaining L_α phase are increased slightly more for POPE-d_{31} (7%) than PDPE-d_{31} (4%). Preferential interaction with polyunsaturated phospholipid is not apparent in these results. The propensity for α-toc to form phase structure with negative curvature that is more tightly packed at the membrane surface, nevertheless, may restrict the contact of free radicals with lipid chains on phosphatidylethanolamine molecules that accumulate polyunsaturated fatty acids.

Key words: α-tocopherol, polyunsaturated fatty acids (PUFA), lipid-lipid interactions, molecular organization, inverted hexagonal H_{II} phase

1. Introduction

Omega-3 polyunsaturated fatty acids[2] (n-3 PUFA) found in fish oil supplements are being increasingly consumed for the many physiological benefits they confer (Mozaffarian and Wu, 2012; Turchini et al., 2012; Calder, 2013; Fuentes et al., 2018, Skulas-Ray et al., 2019). They are characterized by the presence of multiple (≥ 3) cis double bonds that terminate 3 carbons from the terminal methyl (n or ω) end of the chain. Docosahexaenoic acid (DHA, 22:6) with 22 carbons and 6 double bonds is the longest and most unsaturated one (Stillwell and Wassall, 2003). The distinct structure of PUFA causes them to be highly disordered (Feller et al., 2002; Huber et al., 2002) and to modify membrane architecture when taken up into phospholipids, which has been proposed to contribute to their molecular mode of action (Calder, 2012b; Chapkin et al., 2008; Levental et al., 2016; Shaikh, 2012; Wassall et al., 2018). The ease with which a hydrogen atom may be removed from the central methylene group of the repeating $=CH\text{-}CH_2\text{-}CH=$ unit in a PUFA chain means polyunsaturated phospholipids are particularly vulnerable to oxidative attack (Ingold et al., 1993; Raederstorff et al., 2015). Vitamin E is a lipid soluble antioxidant. Its essential role in membranes is to protect lipids against oxidation, and so prevent the structural damage and functional impairment that would result (Traber and Atkinson, 2007; Atkinson et al., 2010). Proposals have been made that vitamin E interacts differentially with polyunsaturated phospholipids in support of this function, although evidence so far is

[2] *Abbreviations:* omega-3 polyunsaturated fatty acid(s) (n-3 PUFA), docosahexaenoic acid (DHA), α-tocopherol (αtoc), phosphatidylcholine (PC), phosphatidylethanolamine (PE), 1-palmitoyl-2-docosahexaenoylphosphatidylethanolamine (PDPE), 1-palmitoyl-2-oleoylphosphatidylethanolamine (POPE), sphingomyelin (SM), oleic acid (OA), 1,2-dimyristoylphosphatidylethanolamine (DMPE), 1,2-oleoylphosphatidylethanolamine (DOPE), 1,2-dioleoylphosphatidylcholine (DOPC), 1-stearoyl-2-oleoylphosphatiylcholine (SOPC), 1-steroyl-2-docosahexaenoylphosphatidylcholine (SDPC), 1,2-dipalmitoylphosphatidylcholine (DPPC)

equivocal (Diplock et al., 1973; Atkinson et al., 2010; Leng et al., 2018). This issue is addressed in the current study.

α-Tocopherol (αtoc) is the form of vitamin E retained in humans (Niki and Traber, 2012). It consists of a chromanol moiety that has a polar hydroxyl group at one end (C-6 position) and a branched phytanyl chain at the other end (C-2 position) (Figure 1). All three (C-5, -7 and -8) positions on the benzene ring are methylated. Studies on αtoc in model membranes, predominantly phosphatidylcholine (PC), in the biologically relevant liquid crystalline phase have established that the hydroxyl group usually resides in the vicinity of the aqueous interface while the phytanyl chain extends towards the hydrophobic interior (Atkinson et al., 2008; Leng et al., 2015; Marquardt et al., 2015 Ausili et al., 2017). The motion of the chain is axially symmetry about the bilayer normal, becoming more disordered and rapid with depth within the bilayer (Ekiel et al., 1988). The effect of αtoc on the surrounding phospholipid molecules is to restrict the motion of their chains - order is increased throughout (Wassall et al., 1986; Leng et al., 2015). A propensity to promote the formation of inverted hexagonal H_{II} phase, in addition, has been reported in the case of phosphatidylethanolamine (PE) (Bradford et al., 2003; Wang and Quinn, 2006). After PC, PE is the second most abundant phospholipid in mammalian membranes (Stillwell, 2016).

Polyunsaturated 1-palmitoyl-2-docosahexaenoylphosphatidylethanolamine (16:0-22:6PE, PDPE) mixed with sphingomyelin (SM) and cholesterol is a model membrane system that we have characterized in a series of studies (Shaikh et al., 2004, 2009; Soni et al., 2008). PDPE was chosen because DHA has been shown to preferentially incorporate into PE (Zerouga et al., 1996). Comparison was made with 1-palmitoyl-2-oleoylphosphatidylethanolamine (16:0-18:1PE, POPE) as a monounsaturated control. Our results from a variety of biophysical methods

demonstrated that an aversion for cholesterol possessed by PUFA drives the sorting of lipids into PDPE-rich/cholesterol-poor (non-raft) and SM-rich/cholesterol-rich (raft-like) nano-sized domains. Indicative of poor affinity for cholesterol, a much smaller increase in order for PDPE than POPE in mixtures with SM was observed following the addition of the sterol by ^{2}H NMR using analogs deuterium labeled throughout the *sn*-1 chain (PDPE-d_{31} and POPE-d_{31}, respectively) (Shaikh et al., 2004). Here we employ a similar approach to distinguish the interactions of αtoc. Solid state ^{2}H NMR spectra were collected comparing the effect of αtoc on PDPE-d_{31} vs. POPE-d_{31} in mixtures with SM (Figure 1).

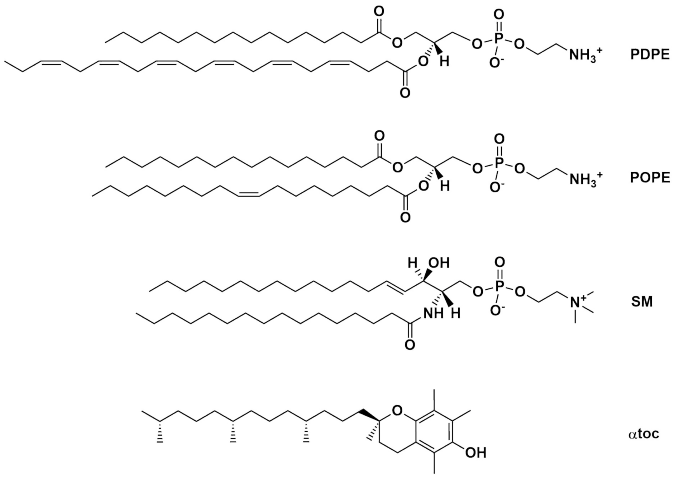

Figure 1 Molecular structure of PDPE, POPE, SM and αtoc.

2. Materials and Methods

2.1 Materials

Egg SM, POPE-d_{31} and PDPE-d_{31} were purchased from Avanti Polar Lipids (Alabaster, AL). αToc was obtained from Cole-Parmer (Vernon Hills, IL) or prepared from commercial α-tocopheryl acetate by hydrolysis (Leng et al., 2015). Cambridge Isotope Laboratories (Andover, MA) was the source for deuterium depleted water.

2.1 Sample Preparation

The procedure was largely as previously described, with precautions taken to minimize the oxidation of the polyunsaturated phospholipid (Soni et al., 2008). SM and POPE-d_{31} or PDPE-d_{31} (1:1 mol), and SM and POPE-d_{31} or PDPE-d_{31} with αtoc (2:2:1 mol) were dissolved in chloroform. Total lipid comprised 30-50 mg. The organic solvent was evaporated using argon gas, followed by vacuum pumping overnight to remove residual solvent. Tris buffer solution (50 mM) was added to the dried lipids (66 wt% hydration), the samples were vortex-mixed and the pH was adjusted to 7.5 with HCl/NaOH. Three lyophilizations were then performed, each in the presence of excess (2 mL) deuterium depleted water to reduce the signal from natural abundance ^{2}HHO. The final samples were rehydrated to 66 wt% (deuterium depleted water), and 3 cycles of freezing and thawing were done to ensure a uniform dispersion. Samples for NMR were transferred to a 5 mm tube that was sealed with a Teflon tape-covered cap.

2.2 ^{2}H NMR Spectroscopy

Spectra were recorded on a homemade solid state NMR spectrometer operating at 46.0 MHz with a 7.05 T super-conducting magnet (Oxford Instruments, Osney Mead, UK) (Kinnun et al., 2018). Pulse programming was achieved with a programmable generator (Sternin, 1985) that was assembled in-house, while signals were acquired in quadrature using a dual-channel digital oscilloscope (R1200 M; Rapid Systems, Seattle, WA). Temperature was maintained to ±0.5°C by a temperature controller (1600 Series; Love Controls, Michigan City, IN). To eliminate spectral distortion due to receiver recovery time, a phase-alternated quadrupolar echo sequence ($90°_x$-τ-$90°_y$-aquire-delay) was implemented (Davis et al., 1976). The parameters were: 90° pulse

width = 3.5 μs; separation between pulses τ = 50 μs; delay between pulse sequences = 1.0 s; sweep width = ±250 kHz (gel phase) or ±100 kHz (liquid-crystalline phase); and typical number of scans = 4096.

2.3 Analysis of NMR Spectra

The first moment was calculated from powder pattern spectra for POPE-d_{31} or PDPE-d_{31} in the mixed membranes with SM and α-toc using

$$M_1 = \frac{\int_{-\infty}^{\infty} |\omega| f(\omega)\, d\omega}{\int_{-\infty}^{\infty} f(\omega)\, d\omega}. \qquad (1)$$

In this equation ω is the frequency relative to the central Larmor frequency and $f(\omega)$ is the line shape (Davis, 1983). The moment is a sensitive indicator of the phase adopted by the deuterium labeled analog of PE.

An additional method of analysis was performed with the FFT depaking algorithm that converts the powder pattern signal for an aqueous dispersion of lipids to a spectrum that corresponds to a sample with a single alignment (McCabe and Wassall, 1997). When applied in the lamellar liquid crystalline L_α phase, the depaked spectrum consists of a superposition of doublets with quadrupolar splitting

$$\Delta\upsilon(\theta) = \frac{3}{2}\left(\frac{e^2qQ}{h}\right)|S_{CD}|P_2(\cos\theta). \qquad (2)$$

Here $\left(\frac{e^2qQ}{h}\right)$ = 168 kHz is the static quadrupolar coupling constant, S_{CD} is the order parameter, $P_2(\cos\theta)$ is the second order Legendre polynomial and θ = 0° is the angle of the normal to the membrane surface relative to the magnetic field. Exploiting the enhancement in spectral resolution, profiles of the gradient of order parameter along the perdeuterated *sn*-1 chain were

generated on the basis of integrated intensity assuming monotonic variation from the top to the bottom of the chain (Lafleur et al., 1989). The order parameter is defined according to

$$S_{CD} = \frac{1}{2}\langle 3cos^2\beta - 1\rangle \qquad (3)$$

where β is the angle that a C-^{2}H bond instantaneously makes with the normal to the lipid-water interface and the angular brackets designate a time average (Seelig, 1977). Values are usually taken in the range $0 \leq |S_{CD}| \leq \frac{1}{2}$. The upper limit reflects fast axial rotation in the all-trans conformation while isotropic motion leads to the lower limit.

3. Results

Solid state ^{2}H NMR spectra were obtained for POPE-d_{31} and PDPE-d_{31} in mixtures with SM (1:1 mol) and with SM and αtoc (2:2:1 mol). The experiments were run from high to low temperature. Reproducibility of data was confirmed over the course of experiments for which the results reported were taken.

3.1 Phase behavior

3.1.1 POPE-d_{31}/SM and PDPE-d_{31}/SM mixtures

^{2}H NMR spectra illustrating the distinction between the phase behavior of POPE-d_{31} and PDPE-d_{31} in 1:1 mol mixtures with SM are shown in Figure 2.

The spectrum for POPE-d_{31}/SM at 0 °C (Fig. 2, left column - top) is indicative of the gel phase. Slow rotational diffusion of the rigid, all-*trans* palmitoyl chain on POPE-d_{31} in the mixed membrane produces a broad featureless spectrum with shoulders at ±63 kHz (Davis, 1983). At 20 °C the spectrum remains gel-like, but a more freely moving chain produces a shift in intensity away from the wings towards the center (Fig. 2, left column - middle). By 37 °C, however, the

spectrum has narrowed dramatically and become a signature for fast axial rotation in the lamellar liquid crystalline phase (Fig. 2, left column - bottom) (Davis, 1983). The palmitoyl chain on POPE-d_{31} has melted so that there is rapid isomerization about C-C bonds. A plateau region of methylene groups with slowly varying order in the upper half of the chain produces the sharp edges at ±17 kHz. Methylene groups with increasingly greater disorder in the bottom half of the chain produce the signals with smaller splitting, culminating in a central signal split by 3 kHz due to the terminal methyl group.

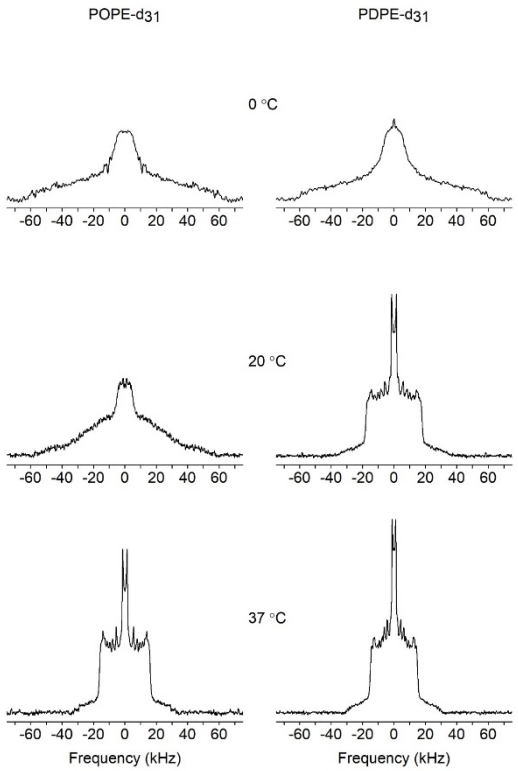

Figure 2 ^{2}H NMR spectra for aqueous dispersion (67 wt% hydration) in 50 mM Tris buffer (pH 7.5) of POPE-d_{31}/SM (1:1 mol) (left column) and PDPE-d_{31}/SM (1:1 mol) (right column). Spectra are symmetrized about the central frequency to enhance signal/noise and are scaled to the same integrated intensity. An expanded re-plot of the spectra at 37 °C is given in Fig. S1.

A change in behavior when DHA replaces oleic acid (OA) is exhibited by the spectra acquired for PDPE-d_{31}/SM mixtures at the same temperatures. The spectrum obtained at 0 °C is, like POPE-d_{31}/SM (Fig. 2, left column - top), characteristic of the gel phase (Fig 2, right column

- top). Unlike POPE-d_{31}/SM (Fig.2, left column - middle), upon increasing the temperature to 20 °C the spectrum for PDPE-d_{31}/SM becomes liquid crystalline in form (Fig. 2, right column - middle). Melting of the palmitoyl chain has occurred and PDPE-d_{31} has undergone the transition from gel to liquid crystalline phase in the mixed membrane with SM. Because polyunsaturated DHA disrupts the regular packing of chains in the gel state more than monounsaturated OA, the temperature for the transition is lowered relative to the mixture containing POPE-d_{31}. As the temperature is increased further to 37 °C, the spectrum retains the same overall shape (Fig. 2, right column - bottom). Increased molecular motion narrows the spectrum and the signals within the spectrum are better resolved. The reduction in frequency of the edges of the spectrum (±15 kHz) and of the splitting the central methyl signal (2 kHz) compared to POPE-d_{31}/SM at the corresponding temperature reflects the disordering effect of DHA.

The spectra for POPE-d_{31}/SM and PDPE-d_{31}/SM in Figure 2 are representative examples. In Figure 3, the first moment M_1 that was calculated (eq. 1) for all the spectra that were recorded between -10 and 50 °C is plotted against temperature to observe phase behavior via the accompanying changes in spectral shape. Slowly decreasing values for the moment at low and high temperature designate gel ($M_1 > 10\times10^4$ s^{-1} for $T < 20$ °C) and liquid crystalline ($M_1 < 7\times10^4$ s^{-1} for $T > 25$ °C) phase, respectively, for POPE-d_{31} mixed with SM (Fig. 3, upper panel). The sharp drop in value between the two temperature regimes that corresponds to the gel to liquid crystalline transition has a mid-point at ~23 °C, which agrees with our earlier work (Shaikh et al., 2004). A qualitatively similar plot is obtained for PDPE-d_{31} mixed with SM (Fig. 3, lower panel). The major difference is a lowering in temperature of the discontinuity in the value of M_1 between gel ($M_1 > 11\times10^4$ s^{-1} for $T < 5$ °C) and liquid crystalline ($M_1 <$

7×10^4 s^{-1} for $T > 10$ °C) states. In agreement with our earlier work, the mid-point is ~7 °C (Shaikh et al., 2004).

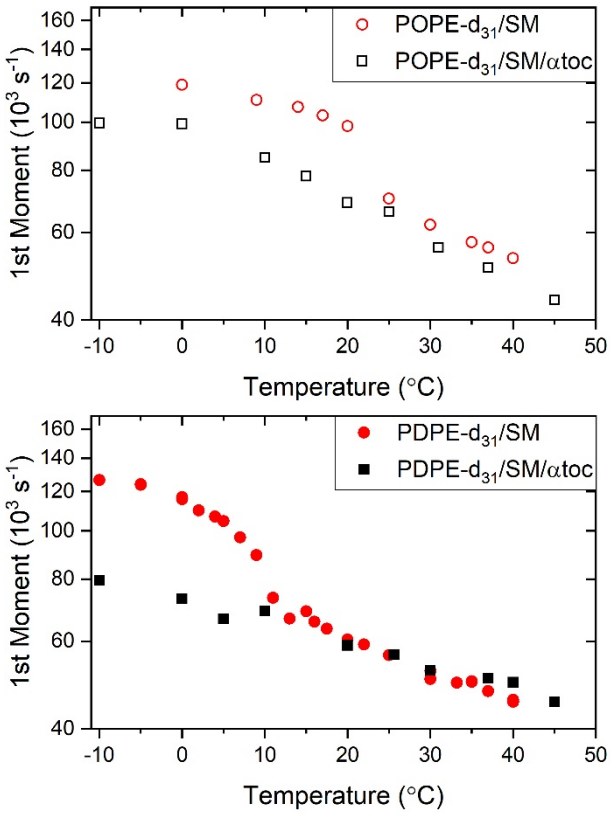

Figure 3 First moment M_1 vs. temperature T for aqueous dispersion (67 wt% hydration) in 50 mM Tris buffer (pH 7.5) of POPE-d_{31}/SM (1:1 mol) and POPE-d_{31}/SM/αtoc (2:2:1 mol) (upper panel), and of PDPE-d_{31}/SM (1:1 mol) and PDPE-d_{31}/SM/αtoc (2:2:1 mol) (lower panel). The scale for M_1 is logarithmic and an uncertainty of ±2% applies to the values.

3.1.2 POPE-d_{31}/SM/αtoc and PDPE-d_{31}/SM/αtoc mixtures

The ^{2}H NMR spectra presented for POPE-d_{31}/SM/αtoc and PDPE-d_{31}/SM/αtoc (2:2:1 mol) in Figure 4 illustrate the effect of αtoc on the phase behavior of POPE-d_{31} and PDPE-d_{31} in the mixtures with SM.

As in the absence of αtoc (Fig. 2, left column - top), gel phase is indicated by the spectrum for POPE-d_{31}/SM/αtoc at 0 °C (Fig. 4, left column - top). A central peak of relatively

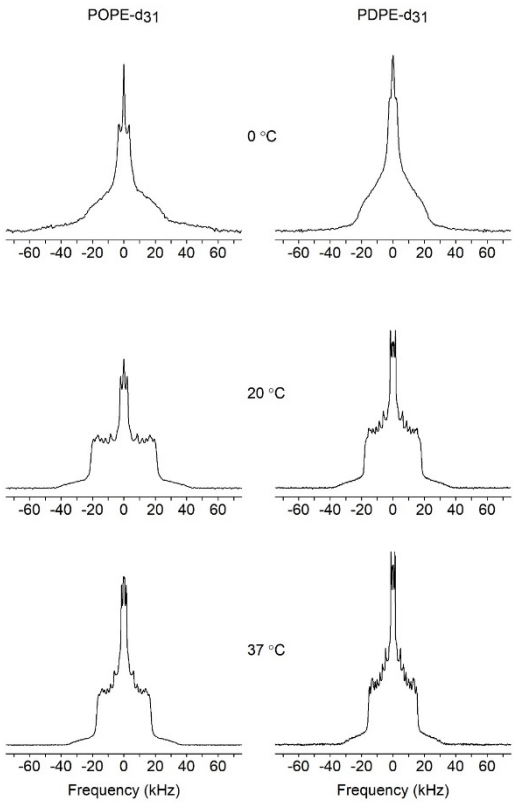

Figure 4 ^{2}H NMR spectra for aqueous dispersion (67 wt% hydration) in 50 mM Tris buffer (pH 7.5) of POPE-d_{31}/SM/αtoc (2:2:1 mol) (left column) and PDPE-d_{31}/SM/αtoc (2:2:1 mol) (right column). Spectra are symmetrized about the central frequency to enhance signal/noise and are scaled to the same integrated intensity. An expanded re-plot of the spectra at 37 °C is given in Fig. S1.

low intensity suggests a small amount of non-lamellar phase is also present. It is apparent that the packing of the palmitoyl chain on POPE-d_{31} is disrupted by αtoc - spectral intensity is lost in the wings and gained in the center of the spectrum. The spectral narrowing due to αtoc, and the disruption to chain packing revealed, is even more dramatic upon raising the temperature to 20 °C. What was a gel-like spectrum without αtoc (Fig. 2, left column - middle) has narrowed to a spectrum that is liquid crystalline in form with αtoc (Fig. 2, left column - middle). In keeping with the further reduction in chain order expected at higher temperature, the spectrum at 37 °C is slightly more decreased in width (Fig. 4, left column - bottom). Close inspection also reveals a pair of signals is now discernible in the central peak that we attribute to inverted hexagonal H_{II} phase (this feature is more clearly seen in an expanded re-plot of the spectrum in Figure S1).

Lamellar phase characterized by sharp edges at ±17 kHz due to the methylene groups in the plateau region of approximately constant order in the upper part of the chain and a pair of signals at ±1.5 kHz due to the terminal methyl groups is responsible for the main body of the spectrum seen here for POPE-d_{31}/SM/ αtoc at 37 °C. Superimposed upon this broad background, a pair of peaks at ±0.3 kHz from terminal methyl groups and a component with edges at ±6 kHz from a plateau region of ordered methylene groups of POPE-d_{31} in H_{II} phase has become resolved. The reduction in splitting with respect to L_α phase is two-fold in origin (Thurmond et al, 1993). Lipid diffusion around the cylindrical structures that comprise H_{II} phase provides another axis for motional narrowing and reduces the splitting by a factor of ½. Greater disorder of lipid chains in H_{II} phase, as previously noted (Thurmond et al., 1993), causes an additional decrease. The resolution of a splitting argues against the formation of cubic phase, we further remark, because lipid diffusion within the highly curved structure of a cubic phase causes a collapse to a single isotropic peak (Yang et al., 2015).

Qualitatively similar spectra were observed for PDPE-d_{31} mixed with SM and αtoc. In common with the mixtures containing POPE-d_{31}, a gel state in which the packing of PDPE-d_{31} is loosened by αtoc is indicated by reduced intensity in the wings of the spectrum at 0 °C for PDPE-d_{31}/SM/αtoc (Fig. 4, right column - top) compared to PDPE-d_{31}/SM (Fig. 2, right column - top). A central peak again suggests the presence of a small amount of non-bilayer phase. At 20 °C, the impact of αtoc is much less dramatic for the DHA- than OA-containing system. The spectrum for POPE-d_{31}/SM that is gel-like (Fig. 2, left column - middle) becomes liquid crystalline-like following the introduction of αtoc (Fig. 4, left column - middle). In contrast, the spectrum for PDPE-d_{31}/SM (Fig. 2, right column - middle) as well as PDPE-d_{31}/SM/αtoc (Fig. 4, right column - middle) is liquid crystalline in form. There is a slight broadening of the edges,

together with a small pair of signals that become resolved in the center (±0.25 kHz) and enhanced intensity in the middle section (~±5 kHz) that we ascribe to H_{II} phase, when αtoc is added. The same changes in response to the introduction of αtoc are exhibited by the spectrum for PDPE-d_{31}/SM/αtoc at 37 °C (Fig. 4, right column - bottom) (re-plotted in Fig. S1 to better distinguish spectral detail).

Figure 3 quantifies the variation in shape with temperature of all the spectra collected for POPE-d_{31}/SM/αtoc (Fig. 3, upper) and PDPE-d_{31}/SM/αtoc (Figure 3, lower) in terms of the first moment. In both cases, the moments decrease continuously throughout the range of temperature plotted. The presence of αtoc prevents tight packing in the gel state, substantially lowering the value of M_1 at low temperature for labeled PE in the mixed membranes so that there is no longer a well-defined discontinuity associated with the melting of chains. That αtoc broadens and depresses the main gel-liquid crystalline phase transition for phospholipid bilayers is well documented (Atkinson et al, 2008).

3.2 Inverted hexagonal H_{II} phase

Figure 5 shows FTT depaked spectra for POPE-d_{31}/SM and PDPE-d_{31}/SM (1:1 mol), and for POPE-d_{31}/SM/αtoc and PDPE-d_{31}/SM/αtoc (2:2:1 mol) at 37 °C. Whereas conventional FFT produces a powder pattern of signals from all orientations relative to the magnetic field, the FFT depake algorithm extracts a single orientation (McCabe et al., 1997). The resultant spectrum consists of series of doublets split according to the degree of anisotropy of the motion undergone by the labeled groups. A substantial enhancement in resolution is so achieved that facilitates spectral analysis.

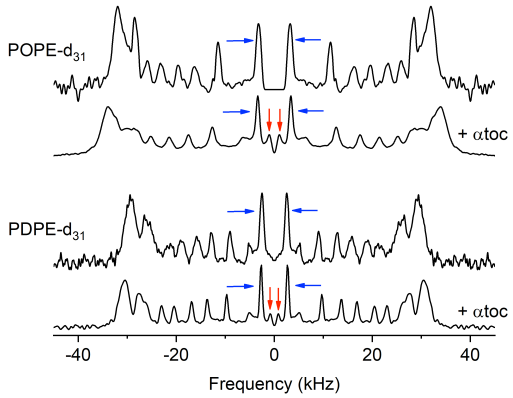

Figure 5 FFT depaked ^{2}H NMR spectra at 37 °C for POPE-d_{31}/SM (1:1 mol) (top) and POPE-d_{31}/SM/αtoc (2:2:1 mol) (upper middle) and for PDPE-d_{31}/SM (1:1 mol) (lower middle) and PDPE-d_{31}/SM/αtoc (2:2:1 mol) (bottom). Doublets assigned to the terminal methyl group on POPE-d_{31} (upper middle) and on PDPE-d_{31} (bottom) in H_{II} (inner splitting - red arrow) and L_α (outer splitting - blue arrow) phase are designated by arrows in the presence of αtoc, whereas in the absence of αtoc there is only a single doublet due to the methyl group on POPE-d_{31} (top) and PDPE-d_{31} (lower middle) in L_α phase (blue arrow). An expanded re-plot of the spectra to better illustrate analysis is given in Fig. S2.

We shall begin by focusing on the signals with small frequency - i.e. the doublets with smallest splitting - due to the disordered terminal methyl groups. There is a just single doublet at ~±3.3 kHz in the depaked spectrum for POPE-d_{31}/SM caused by methyl groups on POPE-d_{31} in lamellar liquid crystalline phase (Fig. 5, top and see Fig. S2). In addition to a lamellar phase signal, a doublet arising from methyl groups on POPE-d_{31} in inverted hexagonal H_{II} phase emerges at ~±1.0 kHz in the depaked spectrum for POPE-d_{31}/SM/αtoc (Fig. 5, upper middle and see Fig. S2). This signal coincides with the spectral component identified earlier in the center of the conventional FFT spectrum for POPE-d_{31}/SM/αtoc (Fig. 4, left column - bottom and see Fig. S1). The advantage conferred by the enhanced resolution of the depaked spectrum is that the signals may be fit (as illustrated in Fig. S2). From the integrated intensity, an approximate estimate of the relative proportion of each phase may then be made. Here in the case of POPE-d_{31}/SM/αtoc, ~20% POPE-d_{31} is H_{II} phase at 37 °C (Table 1).

Membrane composition	% H_{II} phase	$\bar{S}_{CD}$ L_α phase
POPE-d_{31}/SM	0	0.191±0.004
POPE-d_{31}/SM/αtoc	20±6	0.205±0.004
PDPE-d_{31}/SM	0	0.171±0.003
PDPE-d_{31}/SM/αtoc	18±6	0.178±0.004

Table 1 Percentage in H_{II} phase and average order parameter in L_α phae at 37 °C for POPE-d_{31} in POPE-d_{31}/SM (1:1 mol) and POPE-d_{31}/SM/αtoc (2:2:1 mol) and for PDPE-d_{31} in PDPE-d_{31}/SM (1:1 mol) and PDPE-d_{31}/SM/αtoc (2:2:1 mol).

Analogous behavior is exhibited by the depaked spectra for the mixtures containing PDPE-d_{31} at the same temperature. A signal from the methyl groups on PDPE-d_{31} in H_{II} phase, which is not in the spectrum for PDPE-d_{31}/SM without αtoc (Fig. 5, upper middle and see Fig. S2), appears at ~ ±0.8 kHz when αtoc is present in PDPE-d_{31}/SM/αtoc (Fig. 5, lower middle and see Fig. S2). The integrated intensity of this signal corresponds to ~18% H_{II} phase (Table 1). αToc induces the polyunsaturated phospholipid to form about the same amount of H_{II} phase as its monounsaturated counterpart when mixed with SM.

3.3 Acyl Chain Order

We now consider the entire breadth of the depaked spectra recorded at 37 °C to construct profiles of order parameter along the palmitoyl chain of POPE-d_{31} and PDPE-d_{31} that is lamellar phase in the mixed membranes (Fig. 5 and see Fig. S2). Our treatment of the data for POPE-d_{31}/SM and POPE-d_{31}/SM/αtoc outlines the procedure.

The depaked spectrum for POPE-d_{31}/SM, which is solely lamellar phase, consists of a series of signals (Fig. S2, top). They are assigned with increasing frequency to the terminal methyl group that is least ordered, then progressively more ordered individual methylene groups

on moving up the chain and finally a composite of overlapping peaks that represents the plateau region of slowly varying, most ordered methylene groups at the top of the chain. That order decreases monotonically from the top to bottom of a chain is assumed. Relating the frequency to an order parameter via eq. 2, the order parameter profile that is plotted in Figure 6 was obtained for POPE-d_{31} in POPE-d_{31}/SM (Fig. 6, upper panel). It has the form that is characteristic of phospholipids in the lamellar liquid crystalline phase - approximately constant order in the upper portion (positions C2-C8) of chain followed by a drop off of order in the lower portion (positions C9-C16) (Seelig, 1977).

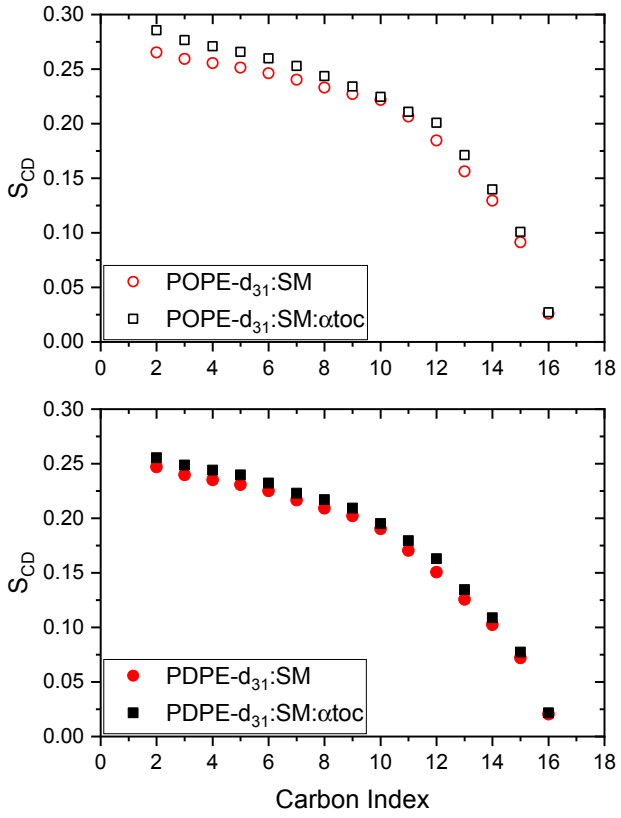

Figure 6 Order parameter profile at 37 °C for POPE-d_{31} in POPE-d_{31}/SM (1:1 mol) and POPE-d_{31}/SM/αtoc (2:2:1 mol) (upper panel) and PDPE-d_{31} in PDPE-d_{31}/SM (1:1 mol) and PDPE-d_{31}/SM/αtoc (2:2:1 mol) (lower panel). A reproducibility of ~±2% applies to the average order parameter $\bar{S}_{CD}$.

As noted earlier, inverted hexagonal phase coexists with lamellar phase following the

addition of αtoc to POPE-d_{31}/SM. Separate peaks from the methyl group on POPE-d_{31} in H_{II} (red line-fit) as well as L_α (blue line-fit) phase become resolved at the low frequency end of the depaked spectrum for POPE-d_{31}/SM/αtoc (Fig. S2, upper middle). Signals from individual methylene groups on POPE-d_{31} in H_{II} phase, however, do not become discernible at higher frequency. They are buried in the noise below the larger peaks (blue line-fits) from the methylene groups on POPE-d_{31} in L_α phase. Although compromised in intensity, the frequency for each of these signals sequentially gives the order parameter for a methylene group on moving up the palmitoyl chain of the component of POPE-d_{31} in the L_α phase. The final composite peak lies outside the frequency range for the H_{II} phase, so it may still be sliced up on the basis of integrated intensity to provide order parameters for the remaining methylene groups in the upper (plateau) region of the chain in lamellar phase. Comparing the depaked spectra for POPE-d_{31}/SM/αtoc (Fig. 5, top and see Fig S2) and POPE-d_{31}/SM (Fig. 5, middle upper and see Fig. S2), it is thus evident that the resonances resolved without αtoc are shifted to larger frequency with αtoc. This shift is reflected in the profile of order parameter for POPE-d_{31} in POPE-d_{31}/SM/αtoc that was generated (Fig. 6, upper panel). αToc elevates order along the whole chain, but does not change the general shape of the profile. There is, in terms of average order parameter, an increase $\Delta\bar{S}_{CD}$ = 0.014 (from $\bar{S}_{CD}$ = 0.191 to 0.205) (Table 1).

The same method of analysis was applied to the depaked spectra for PDPE-d_{31}/SM (Fig. S2, lower middle) and PDPE-d_{31}/SM/αtoc (Fig. S2, bottom). There is an overall reduction in width of the spectra relative to the equivalent mixtures with POPE-d_{31} (Fig. S2, top and upper middle) due to the higher disorder of polyunsaturated PDPE-d_{31}. The reduction in order is displayed in the profiles of order parameter obtained (Fig. 6, lower panel). It is also apparent that although αtoc causes an increase in the order of PDPE-d_{31}, the increase $\Delta\bar{S}_{CD}$ = 0.007 (from $\bar{S}_{CD}$

= 0.171 to 0.178) as quantified by in terms of the average order parameter $\bar{S}_{CD}$ is very small (Table 1).

4. Discussion

Membranes contain a multitude of structurally diverse lipids (Sampaio et al., 2011). Their interactions are fundamental in bringing together membrane constituents (Schmid, 2017). Driven by unequal affinity between different lipids and between lipids and proteins, lipids assemble into lateral patches (domains) of specific composition that provide a local environment necessary for the function of resident proteins. The lipid raft concept is most well developed (Lingwood and Simons, 2010). According to this concept, nano-sized ordered domains (rafts) enriched in sphingolipids and cholesterol serve as the platform for signaling proteins that cross-link and become functional when rafts coalesce. Rafts form because sphingolipids have affinity for cholesterol - the largely linear conformation adopted by the saturated chains on sphingolipids pack well with the rigid steroid moiety of the sterol, which facilitates strong hydrogen bonding between the molecules (García-Arribas et al., 2016). We, and other research groups, have adapted this concept to propose an underlying role for polyunsaturated phospholipids in regulating the size and functionality of rafts (Levental et al., 2016; Kinnun et al. 2018). The basic idea is that polyunsaturated phospholipids have an aversion for cholesterol - highly disordered PUFA chains pack poorly with the steroid moiety (Leng et al., 2018). Polyunsaturated phospholipids consequently segregate into (non-raft) regions depleted in cholesterol, causing rafts to cluster in response to increased disorder relative to rafts (Wassall et al., 2018).

Mixtures of PE with SM are a model membrane system that we have employed to differentiate lipid interactions with cholesterol (Shaikh et al., 2004, 2009; Soni et al., 2008).

Based upon analysis of ^{2}H NMR spectra, supported by the results from complementary biophysical and biochemical methods, it was inferred that PDPE/SM and POPE/SM (1:1 mol) separate into small PE-rich and SM-rich domains (<20 nm in size). This assessment held without and with cholesterol (1:1:1 mol). Emblematic of the aversion cholesterol has for polyunsaturated phospholipids, the increase in order parameter due to cholesterol for PDPE-d_{31} ($\Delta\bar{S}_{CD}\sim0.04$) was very much less than POPE-d_{31} ($\Delta\bar{S}_{CD}\sim0.10$) in the mixed membrane. There is greater partitioning of cholesterol into SM-rich domains and of PE into domains that are depleted in sterol poor for PDPE relative to POPE.

Here we compare ^{2}H NMR spectra for POPE-d_{31}/SM and PDPE-d_{31}/SM mixtures to investigate the partitioning of αtoc. αToc is a lipid soluble antioxidant that is an indispensable membrane constituent of relatively minor concentration (typically < 0.1 mol%) (Wang and Quinn, 1999). Its purpose is to inhibit damage to polyunsaturated phospholipids that are rendered susceptible to oxidative attack by their numerous double bonds. Whether lipid interactions play a role is a longstanding question (Atkinson et al., 2010). ^{2}H NMR spectra recorded for POPE-d_{31}/SM/αtoc and PDPE-d_{31}/SM/αtoc (2:2:1 mol) reveal αtoc moderates the phase behavior of POPE-d_{31} and PDPE-d_{31} in the mixed membranes. In the physiologically relevant liquid crystalline phase, αtoc destabilizes bilayer structure - induces the formation of inverted hexagonal H_{II} phase - and slightly increases membrane order. These effects are comparable with polyunsaturated PDPE and monounsaturated POPE, as summarized in Table 1, which argues against the existence of preferential interaction with polyunsaturated phospholipids. It should be borne in mind, of course, that the experiments were performed at a concentration of vitamin E in excess of that found physiologically (Wang and Quinn, 1999).

4.1 Vitamin E moderates the phase behavior of POPE and PDPE mixed with SM

The ^{2}H NMR spectra for POPE-d_{31}/SM and PDPE-d_{31}/SM in the absence (Fig. 2) and presence of αtoc (Fig. 4) interrogate how the molecular organization of the palmitic acid *sn*-1 chain on POPE-d_{31} and PDPE-d_{31} responds to the introduction of αtoc. At lower temperatures in the gel state, the packing of the chain is disrupted. This point is illustrated by the spectra at 0 °C. Indicative of a reduction in motional constraint, they become narrowed when αtoc is present. The narrowing results in a reduced first moment M_1 (Fig. 3). An abrupt drop in the value of M_1 due to the melting the *sn*-1 chain on POPE-d_{31} and PDPE-d_{31}, which is seen with POPE-d_{31}/SM and PDPE-d_{31}/SM, is then no longer apparent with POPE-d_{31}/SM/αtoc and PDPE-d_{31}/SM/αtoc on raising the temperature. The transition from gel to liquid crystalline state is smeared out beyond detection by αtoc. Adding cholesterol to POPE-d_{31}/SM and PDPE-d_{31}/SM similarly obliterates the transition (Shaikh et al., 2004). A substantial increase in first moment reflecting elevated order at higher temperature in the liquid crystalline state, as well as a decrease reflecting disruption to chain packing at lower temperature in the gel state, is caused by the sterol. By contrast, albeit at smaller concentration (20 vs. 33 mol%), the effect of αtoc on the moment is modest in the liquid crystalline phase - a small reduction in POPE-d_{31}/SM/αtoc and essentially no change or a small increase in PDPE-d_{31}/SM/αtoc. Visual examination of the spectra, however, uncovers more complex behavior. Inverted hexagonal H_{II} phase is induced by αtoc, which will be discussed in the next section.

4.2 Vitamin E destabilizes bilayer structure in PE/SM mixtures

The dynamic molecular shape concept offers a simple rationale for lipid polymorphism. With a small phosphorylethanolamine head group and chains occupying a larger cross-sectional

area, PE molecules have a cone shape that creates negative curvature promoting the formation of inverted hexagonal H_{II} phase (Cullis et al., 1986). The preference for H_{II} phase, as manifest by a reduction in temperature T_h for the transition from lamellar L_α to inverted hexagonal phase, is enhanced by the increase in cross-sectional area that accompanies the higher disorder possessed by unsaturated chains. In the case of POPE-d_{31} and PDPE-d_{31}, plots of first moment vs. temperature exhibit a drop in value that identify values of 65 (Hsueh et al., 2002) and 13 °C (Shaikh et al., 2003), respectively, for the midpoint of the transition.

The ^{2}H NMR spectra recorded for POPE-d_{31}/SM and PDPE-d_{31}/SM (1:1 mol) demonstrate that when mixed with SM in 1:1 mol concentration, POPE-d_{31} and PDPE-d_{31} exist in lamellar phase (Fig. 2). At temperatures where pure PDPE-d_{31} adopts H_{II} phase, it becomes L_α phase following the addition of SM. A simple explanation is provided by the cylindrical shape of SM that, with a bigger phosphorylcholine head group and saturated chains, favors formation of a planar bilayer (Cullis et al., 1986). Mixing SM with PDPE then relieves the negative curvature associated with the conical shape of PE, inducing bilayer structure. Although pure POPE forms L_α phase over the temperature range of the current study, adding SM presumably stabilizes bilayer structure. Mixing PC, which like SM is cylindrical in shape, with PE analogously promotes the transition from H_{II} to L_α phase (Klacslová et al., 2016).

A reversal of the stabilization of bilayer structure conferred by SM is indicated following the introduction of αtoc by the ^{2}H NMR spectra observed with POPE-d_{31}/SM/αtoc and PDPE-d_{31}/SM/αtoc (2:2:1 mol) (Fig. 4). The formation of H_{II} phase in coexistence with L_α phase is revealed by a pair of peaks attributable to the methyl groups on POPE-d_{31} and PDPE-d_{31} that first become resolved in the center of spectra at temperatures > 20 °C in their mixtures with SM and αtoc. They appear to emerge from a central signal indicating the presence of non-bilayer

structure, the nature of which we are unable to specify, at lower temperature. The dynamic molecular shape concept may again be invoked to explain this behavior. αToc is cone-shaped. The hydroxyl head group on the chromanol moiety is small and sits at the aqueous interface, while the disordered phytyl chain that intercalates between phospholipid chains occupies a larger cross-sectional area.

There are earlier reports that αtoc can facilitate the formation of inverted hexagonal phase by PE. Peaks due to H_{II} phase coexisting with L_{α} phase were detected in X-ray scattering intensity profiles for POPE (Wang and Quinn, 2006) and 1,2-dimyristoylphosphatidylethanolamine (DMPE) (Wang et al., 1999) after αtoc was introduced. A propensity to induce H_{II} phase in DMPE and 1,2-dielaidoylphosphatidylethanolamine was observed for αtoc by differential scanning calorimetry (DSC) and ^{31}P NMR (Micol et al., 1990). Analysis of X-ray diffraction data on the H_{II} phase formed by 1,2-oleoylphosphatidylethanolamine (DOPE) revealed greater curvature for the phospholipid monolayer as the content of αtoc was increased (Bradford et al., 2003). The temperature at which H_{II} structure appears, moreover, was found to decrease in X-ray diffraction studies on aqueous dispersions of DOPE/1,2-dioleoylphosphatidylcholine (DOPC) (3:1 mol) following the addition of low (1, 2 and 5 mol%) concentrations of αtoc (Wang and Quinn, 2000). What role a tendency to promote inverted hexagonal phase might play in preventing lipid peroxidation is unclear. We speculate that the tighter packing at the surface associated with negative curvature would limit the penetration of free radicals into the membrane (Li et al., 2000). It is interesting, thus, to note that DHA is found to accumulate in PE more than PC (Wassall and Stillwell, 2008).

With the superior resolution bestowed by depaking, the relative amount of POPE-d_{31} in POPE-d_{31}/SM/atoc and of PDPE-d_{31} in PDPE-d_{31}/SM/atoc that adopts H_{II} vs. L_{α} phase was

estimated from the integrated intensity of separate signals assigned to the methyl group on the *sn*-1 chain of POPE-d_{31} and PDPE-d_{31} in the two phases (Fig. 5). The fraction of H_{II} phase determined in this way for POPE-d_{31} (~20%) and PDPE-d_{31} (~18%) at 37 °C is identical within experimental error (20±6% vs.18±6%) (Table 1). Order parameter profiles constructed from the depaked data furthermore demonstrate that αtoc raises the order for the palmitoyl chain of POPE-d_{31} and PDPE-d_{31} that retains L_α phase structure in POPE-d_{31}/SM/αtoc and PDPE-d_{31}/SM/αtoc, respectively. (Fig. 6). Although the increase in average order parameter $\bar{S}_{CD}$ is almost twice as big for POPE-d_{31} (7%) as for PDPE-d_{31} (4%), it should be borne in mind that the difference ($\Delta\bar{S}_{CD} = 0.014 \pm 0.006$ vs. 0.007 ± 0.005) borders on experimental uncertainty (Table 1). The values compare with increases of 15-20% (Wassall et al., 1986; Suzuki et al., 1983) and 5-10% (Leng et al., 2015) in $\bar{S}_{CD}$ that were measured when the same concentration of αtoc was added to bilayers composed only of a saturated PC and an unsaturated or polyunsaturated PC, respectively. To the best of our knowledge, order parameters have not been reported for PE bilayers containing αtoc.

4.3 Concluding remarks

Does favorable interaction with polyunsaturated phospholipids heighten the local concentration of αtoc close to the lipid species most susceptible to free radical attack? This question continues to be debated (Shaikh et al., 2015; Atkinson et al., 2019; Zing and Meydani, 2019). Such an arrangement would certainly be advantageous in preventing oxidation. DSC scans for PDPE/SM (1:1 mol) mixtures offer some support (Stillwell, 2006). They display two transitions - at lower and higher temperature due to phase rich in, respectively, PDPE and SM. When 1, 5 and 10 mol% αtoc were added, a much greater reduction in enthalpy was observed for

the transition at lower temperature (PUFA-rich) than the transition at higher temperature (SM-rich) that was almost unaffected. Preferential affinity of αtoc for polyunsaturated PDPE over saturated SM is implied. How much the phase behavior of PDPE-d_{31} or POPE-d_{31} relative to SM is affected by αtoc cannot be decided in the current work. The similarity in the effect of αtoc on POPE-d_{31} vs. PDPE-d_{31} in 1:1 mol mixtures with SM seen does not indicate greater interaction with the PUFA-containing lipid. Indeed, the changes in molecular organization tend to be greater for monounsaturated POPE-d_{31}.

MD simulations have recently begun to address how vitamin E organizes in membranes (Quin and Yu, 2011; Leng et al., 2015; Boonnoy et al., 2018). Consistent with the slight preference indicated for POPE over PDPE in mixed membranes with SM, higher binding energy for αtoc was measured in 1-stearoyl-2-oleoylphosphatiylcholine (18:0-18:1PC, SOPC) than 1-steroyl-2-docosahexaenoylphosphatidylcholine (18:0-22:6PC, SDPC) bilayers by umbrella sampling in all-atom (AA) simulations (Leng et al., 2018). From coarse-grained (CG) simulations on a bilayer made of saturated 1,2-dipalmitoylphosphatidylcholine (16:0-16:0PC, DPPC) and unsaturated DOPC in 1:1 mol ratio, it was deduced that αtoc prefers DPPC (Muddana et al., 2012). The boundary between DPPC-rich and DOPC-rich domains, intriguingly, was where the vitamin was found predominantly.

In summary, the results in this study show that αtoc induces H_{II} phase and slightly increases the order of POPE-d_{31} and PDPE-d_{31} in mixed membranes with SM. Since PDPE-d_{31} is not affected more than POPE-d_{31}, preferential interaction of vitamin E with a polyunsaturated phospholipid is not implied. The more closely packed aqueous interface implied by a propensity to induce H_{II} phase does have the potential to restrict free radicals entering the hydrophobic interior and so inhibit the oxidation of PE into which PUFA are often taken up.

Acknowledgements

We appreciate the funding of the IUPUI URM Program by the NSF (DBI-1041184).

Author contributions

A.T.C. performed experiments, analyzed data and wrote the manuscript, J.J.K. performed experiments, analyzed data and contributed to the writing of the manuscript, J.A.W. performed experiments and was involved in the inception of the project, and S.R.W. wrote the manuscript and takes primary responsibility for the research.

Appendix A. Supplementary data

Supplementary data associated with this article can be found, in the online version, at xxx.

References

Atkinson, J., Epand, R.F., Epand, R.M., 2008. Tocopherols and tocotrienols in membranes: a critical review. Free Rad. Biol. Med. 44, 739-764.

Atkinson, J., Harroun, T., Wasssall, S.R., Stillwell, W., Katsaras, J., 2010. The location and behavior of α-tocopherol in membranes. Mol. Nutr. Food Res. 54, 641-651.

Atkinson, J., Marquardt, D., Harroun, T., 2019. The behavior of vitamin E in menbranes. In: Niki, E. (Ed.), Vitamin E: Chemistry and Nutritional Benefits. The Royal Society of Chemistry, London, pp. 32-50.

Ausili, A., de Godos, A. M., Torrecillas, A., Aranda, F.J., Corbalán-García, S., Gómez-Fernández, J.C., 2017. The vertical location of α-tocopherol in phosphatidylcholine membranes is not altered as a function of the degree of unsaturation of the fatty acyl chains. Phys. Chem. Chem. Phys. 19, 6731-6742.

Boonnoy, P., Karttunen, M., Wong-ekkabut, J., 2018. Does α□tocopherol flip-flop help to protect membranes against oxidation? J. Phys. Chem. B 122, 10362-10370.

Bradford, A., Atkinson, J., Fuller, N., Rand, R.P., 2003. The effect of vitamin E on the structure of membrane lipid assemblies. J. Lipid Res. 44, 1940-1945.

Calder, P.C., 2012a. Omega-3 polyunsaturated fatty acids and inflammatory processes: nutrition or pharmacology? Brit. J. Clin. Pharmacol. 75, 645-662.

Calder, P.C., 2012b. Mechanisms of action of (n-3) fatty acids, J. Nutr. 142, 592S–599S.

Chapkin, R.S., Wang, N., Fan, Y.Y., Lupton, J.R., Prior, I.A., 2008. Docosahexaenoic acid alters the size and distribution of cell surface microdomains. Biochim. Biophys. Acta 1778, 466–471.

Cullis, P.R., Hope, M.J., Tilcock, C.P.S., 1986. Lipid polymorphism and the roles of lipids in membranes. Chem. Phys. Lipids 40, 127-144.

Davis, J.H., Jeffery, K.R., Bloom, M., Valic, M.I., Higgs, T.P., 1976. Quadrupolar echo deuteron magnetic resonance spectroscopy in ordered hydrocarbon chains. Chem. Phys. Lett. 42, 390–394.

Davis, J.H., 1983. The description of lipid conformation, order and dynamics by ^{2}H NMR. Biochim. Biophys. Acta 737, 117-171.

Diplock, A.T., Lucy, J.A., 1973. The biochemical modes of action of vitamin E: a hypothesis. FEBS Lett. 29, 205-210.

Ekiel, I.H., Hughes, L., Burton, G.W., Jovall, P.Å., Ingold, K.U. and Smith, I.C.P., 1988. Structure and dynamics of α-tocopherol in model membranes and in solution: A broad-line and high-resolution NMR study. Biochemistry 27, 1432-1440.

Feller, S.E., Gawrisch, K., MacKerrell Jr., A.D., 2002. Polyunsaturated fatty acids in lipid bilayers: intrinsic and environmental contributions to their unique physical properties. J. Am. Chem. Soc. 124, 318–326.

Fuentes, N., Kim, E., Fan, Y.Y., Chapkin, R.S., 2018. Omega-3 fatty acids, membrane remodeling and cancer prevention. Mol. Aspects Med. 64, 79-91.

García-Arribas, A.B., Alonso, A., Goñi, F.M., 2016. Cholesterol interactions with ceramide and sphingomyelin. Chem. Phys. Lipids 199, 26–34.

Hsueh, Y., Weng, C., Chen, M., Thewalt, J., Zuckermann, M., 2010. Deuterium NMR Study of the Effect of Ergosterol on POPE Membranes. Biophys. J. 98, 1209-1217.

Huber, T., Rajamoorthi, K., Kurze, V.F., Beyer, K., Brown, M.F., 2002. Structure of docosahexaenoic acid-containing phospholipid bilayers as studied by ^{2}H NMR and molecular dynamics simulations. J. Am. Chem. Soc. 124, 298–309.

Ingold, K.U., Bowry, V.W., Stocker, R., Walling, C., 1993. Autoxidation of lipids and

antioxidation by α-tocopherol and ubiquinol in homogeneous solution and in aqueous dispersions of lipids: unrecognized consequences of lipid particle size as exemplified by oxidation of human low density lipoprotein. Proc. Natl. Acad. Sci. USA 90, 45-49.

Kinnun, J.J., Bittman, R., Shaikh, S.R., Wassall, S.R., 2018. DHA modifies the size and composition of raftlike domains: A solid-state ^{2}H NMR study. Biophys. J. 114, 380-391.

Klacslová, M., Botá, A., Balgavý, P. 2016. DOPC-DOPE composition dependent L_{α}-H_{II} thermotropic phase transition: SAXD study. Chem. Phys. Lipids 198, 46-50.

Lafleur, M., Fine, B., Sternin, E., Cullis, P.R., Bloom, M., 1989. Smoothed orientational order profile of lipid bilayers by ^{2}H-nuclear magnetic resonance. Biophys. J. 56, 1037-1041.

Leng, X., Kinnun, J.J., Marquardt, D., Ghefli, M., Kucerka, N., Katsaras, J., Atkinson, J., Harroun, T.A., Feller, S.E., Wassall, S.R., 2015. α-Tocopherol is well designed to protect polyunsaturated phospholipids: MD simulations. Biophys. J. 109, 1608-1618.

Leng, X., Kinnun, J. J., Marquardt, D., Ghefli, M., Kucerka, N., Katsaras, J., Atkinson, J., Harroun, T. A., Feller, S. E., Wassall, S. R., 2015. α-Tocopherol is well designed to protect polyunsaturated phospholipids: MD simulations. Biophys. J. 109, 1608-1618.

Leng, X., Zhu, F. Wassall, S.R., 2018. Vitamin E has reduced affinity for a polyunsaturated phospholipid. J. Phys. Chem. B 122, 8351-8358.

Leng, X., Kinnun, J.J., Cavazos, A.T., Canner, S.W., Shaikh, S.R., Feller, S.E.,and Wassall, S.R., 2018. All n-3 PUFA are not the same: MD simulations reveal differences in membrane organization for EPA, DHA and DPA. Biochim. Biophys. Acta 1860, 1125-1134.

Levental, K.R., Lorent, J.H., Lin, X., Skinkle, A.D., Surma, M.A., Stockenbojer, E.A., Gorfe, A.A., Levental. I., 2016. Polyunsaturated lipids regulate membrane domain stability by tuning membrane order. Biophys. J. 110, 1800–1810.

Li, Q-T., Yeo, M.H., Tan, B.K., 2000. Lipid peroxidation in small and large phospholipid unilamellar vesicles induced by water-soluble free radical sources. Biochem. Biophys. Res. Commun. 273, 72–76.

Lingwood, D., Simons, K., 2010. Lipid rafts as a membrane-organizing principle. Science 327, 46-50.

Marquardt, D., Kučerka, N., Katsaras, J., Harroun, T.A., 2015. α-Tocopherol's location in membranes is not affected by their composition. Langmuir 31, 4464-4472.

McCabe, M.A., Wassall, S.R., 1997. Rapid deconvolution of NMR powder spectra by weighted fast Fourier transformation. Solid State Nucl. Magn. Reson. 10, 53-61.

Micol, V., Aranda, F.J., Villalain, J. and Juan C. G6mez-Fernández, J.C., 1990. Influence of vitamin E on phosphatidylethanolamine lipid polymorphism. Biochim. Biophys. Acta 1022, 194-202.

Mozaffarian, D., Wu, J.H.Y., 2012. (n-3) Fatty acids and cardiovascular health: are effects of EPA and DHA shared or complementary? J. Nutr. 142, 614S-625S.

Muddana, H.S., Chiang, H.H., Butler, P.J., 2012. Tuning membrane phase separation using nonlipid amphiphiles. Biophys. J. 102, 489-497.

Niki, E., Traber, M.G., 2012. A history of vitamin E. Ann. Nutr. Metab. 61, 207-212.

Raederstorff, D., Wyss, A., Calder. P.C., Weber, P., Eggersdorfer, M., 2015. Vitamin E function and requirements in relation to PUFA. Brit. J. Nutr. 114, 1113–1122.

Qin, S-S., Yu, Z-W., 2011. Molecular dynamics simulations of α-tocopherol in model membranes. Acta Phys. - Chim. Sin. 27, 213-227.

Sampaio, J.L., Gerl, M.J., Klose, C., Ejsing, C.S., Beug, H., Simons, K., Shevcheko, A., 2011. Membrane lipidome of an epithelial cell line. Proc. Natl. Acad. Sci. USA 108, 1903-1907.

Schmid, F., 2017. Physical mechanisms of micro- and nanodomain formation in multicomponent lipid membranes. Biochim. Biophys. Acta 1859, 509-528.

Seelig, J., 1977. Deuterium magnetic resonance: theory and application to lipid membranes. Q. Rev. Biophys. 10, 353-418.

Shaikh, S.R., Cherezov, V., Caffery, M., Stillwell, W., Wassall, S.R., 2003. Interaction of Cholesterol with a Docosahexaenoic Acid-Containing Phosphatidylethanolamine: Trigger for Microdomain/Raft Formation? Biochemistry 42, 12028-12037.

Shaikh, S.R., Dumaual, A.C., Castillo, A., LoCascio, D., Siddiqui, R.A., Stillwell, W., Wassall, S.R., 2004. Oleic and docosahexaenoic acid differentially phase separate from lipid raft molecules: a comparative NMR, DSC, AFM, and detergent extraction study. Biophys. J. 87, 1752-1766.

Shaikh, S.R., Locascio, D.S., Soni, S.P., Wassall, S.R., Stillwell, W., 2009. Oleic- and docosahexaenoic acid-containing phosphatidylethanolamines differentially phase separate from sphingomyelin. Biochim. Biophys. Acta 1788, 2421-2426.

Shaikh, S.R., 2012. Biophysical and biochemical mechanisms by which dietary N-3 polyunsaturated fatty acids from fish oil disrupt membrane lipid rafts. J. Nutr. Biochem. 23, 101-105.

Shaikh, S.R., Wassall, S.R., Brown, D.A., Kosaraj, R., 2015. n-3 Polyunsaturated fatty acids, lipid clusters and vitamin E. Curr. Top. Membr. *75*, 209-231.

Soni, S.P., LoCascio, D.S., Liu, Y., Williams, J.A., Bittman, R., Stillwell, W., Wassall, S.R., 2008. Docosahexaenoic acid enhances segregation of lipids between raft and non-raft domains: ^{2}H-NMR study. Biophys. J. 95, 203-214.

Sternin, E., 1985. Data acquisition and processing: a systems approach. Rev. Sci. Instrum. 56,

2043–2049.

Stillwell, W., Wassall, S.R., 2003. Docosahexaenoic acid: membrane properties of a unique fatty acid. Chem. Phys. Lipids 126, 1-27.

Stillwell, W., 2006. The role of polyunsaturated lipids in membrane raft function. Scand. J. Food Nutr. 50, 107-113.

Stillwell, W., 2016. An Introduction to Biological Membranes, Second Edition. Elsevier Science, Amsterdam, the Netherlands.

Skulas-Ray, A.C., Wilson, P.W.F, Harris, W.S., Brinton, E.A., Kris-Etherton, P.M., Richter, C.K., Jacobson, T.A., Engler, M.B., Miller, M., Robinson, J.G., Blum, C.B., Rodriguez-Leyva, de Feranti, S.D., Welty, F.K., 2019. Omega-3 fatty acids for the management of hypertriglyceridemia. A science advisory from the American Heart Association. Circulation 140, e673–e691.

Suzuki, Y.J., Tsuchiya, M., Wassall, S.R., Choo, Y.M., Govil, G., Kagan, V.E., Packer, L., 1993. Structural and dynamic membrane properties of α-tocopherol and α-tocotrienol: implication to the molecular mechanism of their antioxidant potency. Biochemistry 32, 10692-10699.

Thurmond, R.L., Lindblom, G., Brown, M.F., 1993. Curvature, order, and dynamics of lipid hexagonal phases studied by deuterium NMR spectroscopy. Biochemistry 32, 5394-5410.

Traber, M.G., Atkinson, J., 2007. Vitamin E, antioxidant and nothing more. Free Rad. Biol. Med. 43, 4-15.

Turchini, G.M., Nichols, P.D., Barrow, C., Sinclair, A.J., 2012. Jumping on the omega-3 bandwagon: distinguishing the role of long-chain and shortchain omega-3 fatty acids. Crit. Rev. Food Sci. Nutr. 52, 795–803.

Wang, X., Quinn, P.J., 1999. Vitamin E and its function in membranes. Prog. Lipid Res. 38, 309-

336.

Wang, X., Quinn, P.J. 2000. The distribution of α-tocopherol in mixed aqueous dispersions of phosphatidylcholine and phosphatidylethanolamine. Biochim. Biophys. Acta 1509, 361-372.

Wang, X., Quinn, P.J., 2006. The structure and phase behaviour of α-tocopherol-rich domains in 1-palmitoyl-2-oleoyl-phosphatidylethanolamine. Biochimie 88, 1883-1888.

Wassall, S.R., Thewalt, J.L., Wong, L., Gorrissen, H., Cushley, R.J., 1986. Deuterium NMR study of the interaction of α-tocopherol with a phospholipid model membrane. Biochemistry 26, 319-326.

Wassall, S.R., Stillwell, W., 2008. Docosahexaenoic acid domains: the ultimate non-raft membrane domain. Chem. Phys. Lipids 153, 57-63.

Wassall, S.R., Leng, X., Canner, S.W., Pennington, E.R., Kinnun, J.J., Cavazos, A.T., Dadoo, S., Johnson, D., Heberle, F.A., Katsaras, J., Shaikh, S.R., 2018. Docosahexaenoic acid regulates the formation of lipid rafts: A unified view from experiment and simulation. Biochim. Biophys. Acta 1860, 1985-1993.

Yang, Y., Yao, H., Hong, M. 2015. Distinguishing bicontinuous lipid cubic phases from isotropic membrane morphologies using ^{31}P solid-state NMR spectroscopy. J. Phys. Chem. B 119, 4993-5001.

Zerouga, M., Stillwell, W., Stone, J., Powner, A., Dumaual, A.C., Jenski, L.J., 1996. Phospholipid class as a determinant in docosahexaenoic acid's effect on tumor cell viability. Anticancer Res. 16, 2863–2868.

Zing, J-M., Meydani, M., 2019. Interactions between vitamin E and polyunsaturated fatty acids. In: Weber, P., Birringer, M., Blumberg. J., Eggersdorfer, M., Frank, J. (Eds.), Vitamin E in Human Health. Nutrition and Health. Humana Press, Cham, pp. 141-159.